

## Determination of Corrosion and Adsorption Parameters of 1, 3, 4-thiadiazole-2, 5-dithiol on ASTM A-890-1B Stainless Steel in 3.5% NaCl Solution

M. Guzmán\*, R. Lara and L. Vera

Departamento de Químicas, Facultad de Ciencias, Universidad Católica del Norte, Antofagasta-CHILE

\*E-mail: [mguzman@ucn.cl](mailto:mguzman@ucn.cl)

Received: 23 July 2013 / Accepted: 19 August 2013 / Published: 25 September 2013

---

Using the electrochemical linear polarization resistance technique, 1,3,4-thiadiazole-2,5-dithiol corrosion current density of ASTM A-890-1B steel is determined in a 3.5% NaCl solution at different temperatures. The corrosion inhibition process is mixed. Apparent activation energy is calculated, being the one with inhibitor slightly greater than that without it. The isotherm is better adjusted to the experimental data was Flory-Huggins, with three molecules of water removed from the alloy surface by the adsorbed molecule inhibitor; this also is reflected by calculating the surface these. Normal thermodynamic adsorption parameters are calculated, showing that the process is spontaneous and exothermic. Inhibitor adsorption on the stainless steel surface is a chemical adsorption.

---

**Keywords:** inhibitor corrosion, ASTM A-890-1B Stainless Steel, adsorption isotherm, 1, 3, 4-thiadiazole-2, 5-dithiol

### 1. INTRODUCTION

In general, some organic molecules have shown great effectiveness in inhibiting aqueous corrosion in a great variety of metals and alloys [1,2]. The adsorption of these metals is generally explained by the formation of a film on the metal surface. Inhibitor adsorption can prevent cathodic and anodic reactions or both together. This inhibition may be a chemical or physical adsorption. This effect is obtained through the formation of a diffusion barrier or by blocking reaction sites [3,4]. The electrostatic attraction between the charged inhibitor molecule and the active charged sites on the metal surface result in physical adsorption. The literature shows that most organic inhibitors are adsorbed on the metal by surface water molecule displacement, forming a compact barrier [3].

Molecules containing nitrogen and sulfur in their structures are good inhibitors, as compared to compounds that only contain sulfur or nitrogen [5].

The inhibition property of these compounds is attributed to their molecular structure. The planarity and pairs of free electrons in heteroatom are important characteristics that determine the adsorption of these molecules on the metal surface [4]. Heterocyclic compounds containing sulfur and nitrogen are good corrosion inhibitors in aggressive mediums [5, 6, 7-9].

There are currently stainless steel alloys highly resistant to corrosion such as duplex ASTM A-890-1B stainless steels, this duplex stainless steels have a chemical composition carefully adjusted to obtain a mixed crystalline structure of about half a ferritic phase and half an austenitic phase. This is possible due to the addition of ferritic steel and a small controlled amount of nickel (sometimes Mn and N). The resulting alloy shows mechanical characteristics much better than those of austenitic steel, allowing the use of fewer thicknesses and thus saving material. In addition, good resistance to uniform and localized corrosion such as pitting, crevice or cracking is obtained. Very good results have been reported for some of the most critical cases such as high chloride concentration and the presence of reducing agents and hydrogen sulfide<sup>4</sup>. This duplex stainless steels, it has been studied using 5-amino-1,3,4-thiadiazole-2-thiol inhibitor of the corrosion in a 3.5% NaCl solution [10].

The 1,3,4-thiadiazole-2,5-dithiol (bismuthiol), forms polymers with metals [11], and there are several patents of this compound as corrosion inhibitor [12,13]. This compound has been studied like corrosion inhibitor of copper [14,15].

The objective of this work is to study the effect like inhibitor of 1,3,4-thiadiazole-2,5-dithiol and determining adsorption parameters on stainless steels ASTM A-890-1B in 3,5% a NaCl solution.

## 2. EXPERIMENTAL

### 2.1. Materials

The stainless steel Duplex ASTM A-890-1B has the following compositions in %

**Table 1.** Composition of steel in study

C	N	Si	P	S	Cr	Mn	Fe	Ni	Cu	Mo
0.04	0.15	1.0	0.04	0.04	25.0	1.0	bal	5.5	3.0	1.82

Resistance of stainless steel to pitting and crevice corrosion is improved by chromium, molybdenum and nitrogen addition. Using the pitting resistance equivalent numbers (PREN), is a number indicating the resistance of stainless steel to pitting corrosion related to chemical composition and derived from the equation,

$$\text{PREN} = \% \text{Cr} + 3.3 \% \text{Mo} + 16 \% \text{N} \quad (\text{eq 1})$$

In the case of the ASTM-890 the obtained value was about 33.4, value PREN between 30-50, they are resistant of pitting in water sea, they indicate that our steel in the study they are resistant to the pitting [16,17]. Figure 1 shows the 1,3,4-Thiadiazole-2,5-dithiol inhibitor molecule structure (Aldrich 98%).

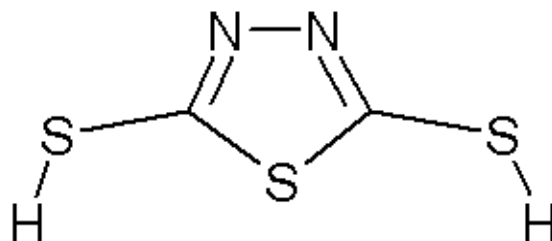


**Figure 1.** 1,3,4-Thiadiazole-2,5-dithiol structure.

*Pretreatment.* ASTM A-890-1B Stainless Steel is annealed at 400°C for 2 h and then air-cooled.

## 2.2. Electrodes

The working electrode was prepared on an ASTM A-890-1B pretreated cylinder connected to a copper conductor wire. The cylindrical part was isolated with epoxy resin, leaving a 0.21 cm<sup>2</sup> exposed area. Before each experiment the exposed area of the working electrode was treated with soft 3M 1500 sand paper, to a metallic shine. Then it was brushed carefully, washed with distilled water, degreased with ethanol, and finally dried with soft paper.

The reference electrode was saturated calomel (SCE), which was cleaned before each experiment to avoid inhibitor contamination. It was externally cleaned with distilled water and dried with soft paper, keeping some KCl crystals inside. The auxiliary electrode was a platinum cylinder with a 1.77 cm<sup>2</sup> exposed surface. Before each experiment it was cleaned with distilled water, degreased with ethanol, rinsed again with bi-distilled water, and dried with soft paper.

## 2.3. Measurement system

Fifty mL of 3.5% NaCl electrolyte, with and without inhibitor, is introduced into the electrochemical cell and kept at constant temperature (288.2, 293.2, 298.2, 303.2, 308.2, 313.2 K), the working electrode was kept inside the cell for 60 min. Then the auxiliary electrode was introduced into the cell, facing (at the same height) the working electrode at 2-3 mm apart. The electrolyte was sucked into the Luggins' capillary and the reference electrode was put in place.

Potentiodynamic measures were taken after a 30-min period of working electrode immersion into 3.5% NaCl at different 1,3,4-Thiadiazole-2,5-dithiol concentrations ( $5 \times 10^{-5}$  M;  $10 \times 10^{-5}$  M;  $20 \times$

$10^{-5}$  M;  $30 \times 10^{-5}$  M;  $50 \times 10^{-5}$  M). The cell was connected to a Radiometer PGZ 301 Potentiostat, and the scanning speed was fixed at 60 mV/s.

Possible orientation of 1,3,4-thiadiazole-2,5-dithiol on ASTM A-890-1B stainless surface is analyzed, calculating area using Weblab ViewwerPro 4.0 and ACD/ChemSketch 10.02.

### 3. RESULTS AND DISCUSSION

#### 3.1. Polarization curves

**Table 2.** Potentiodynamic polarization parameters of 1,3,4-thiadiazole-2,5-dithiol on ASTM A-890-1B stainless steel in an NaCl 3.5% aqueous solution.

Concentration (mol dm <sup>-3</sup> ) 10 <sup>5</sup>	<i>i</i> <sub>corr</sub> (μA/cm <sup>2</sup> )	E (%)	E <sub>corr</sub> ECS(mV)	<i>b</i> <sub>a</sub> (mV/dec)	- <i>b</i> <sub>c</sub> (mV/dec)
<b>288.2 K</b>					
0	663	-	-1162.7	51.80	33.50
5	278	58.1	-1094.3	202.5	82.30
10	222	66.5	-1070.1	289.2	96.20
20	179	73.0	-1054.5	271.7	94.80
30	150	77.4	-1057.3	278.2	93.40
50	125	81.1	-1058.4	265.4	92.80
<b>293.2 K</b>					
0	713	-	-1134.2	84.80	52.40
5	314	56.0	-1054.3	260.3	92.7
10	247	65.4	-1075.2	264.2	93.70
20	205	71.3	-1049.6	267.1	93.90
30	172	75.9	-1060.2	257.2	93.10
50	141	80.2	-1060.5	260.7	92.00
<b>298.2 K</b>					
0	760	-	-1153.2	67.10	36.90
5	344	54.8	-1150.2	215.5	85.45
10	279	63.3	-1075.3	219.6	89.10
20	234	69.2	-1059.3	202.4	84.60
30	193	74.7	-1054.9	208.3	87.80
50	160	78.9	-1060.5	260.7	92.01
<b>303.2 K</b>					
0	810	-	-1119.9	133.3	63.10
5	382	52.8	-1048.8	230.2	91.5
10	311	61.6	-1055.0	231.1	94.3
20	260	67.9	-1064.9	244.5	95.2
30	215	73.4	-1034.5	278.3	104.1
50	192	76.2	-1084.7	184.4	85.0
<b>308.2 K</b>					
0	867	-	-1134.1	95.50	63.40
5	420	51.6	-1074.6	221.3	91.6
10	349	59.7	-1065.6	231.5	92.6
20	293	66.2	-1050.0	225.2	94.2
30	247	71.5	-1048.6	235.2	96.3
50	216	75.1	-1052.0	234.3	98.3
<b>313.2 K</b>					
0	923	-	-1093.2	155.6	84.70
5	454	50.8	-1039.7	255.6	102.5
10	383	58.5	-1054.8	274.9	103.6
20	319	65.4	-1060.2	265.1	96.9
30	278	69.9	-1062.3	258.2	97.9
50	231	74.9	-1060.6	172.4	86.2

The results of polarization corrosion parameters as a function of inhibitor and temperature concentration are summarized in Table 2. In this table shows that the greater the inhibitor concentration the greater its efficiency, regardless of temperature. Inhibitor efficiency is given by

$$E\% = \frac{[i_c - i_{c(inh)}]}{i_c} \tag{eq 2}$$

where  $i_c$  is corrosion current density without inhibitor and  $i_{c(inh)}$  is corrosion current density with an inhibitor. The efficiency of a certain inhibitor concentration remains almost steady at different temperatures.

Maximum compound solubility is  $5 \times 10^{-4}$  in a 3.5% NaCl solution which, if greater, would allow a higher degree of covering. In the corrosion medium there may be competition between active ions such as  $Cl^-$  and the inhibitor molecules due to adsorption on the metal surface. Adsorption will depend on the relative concentration of each of them. This means that the inhibitory effect of the organic molecules will depend the  $Cl^-$  concentration, which decreases as the inhibitory capacity to form a protective layer on the metal surface increases.

$E_{corr}$  is almost steady. Regarding the curve without the inhibitor, Tafel slopes change positively and negatively for the anodic and cathodic processes, respectively, that is, the inhibitory influences the two processes and behaves in a mixed fashion.

### 3.2. Kinetic

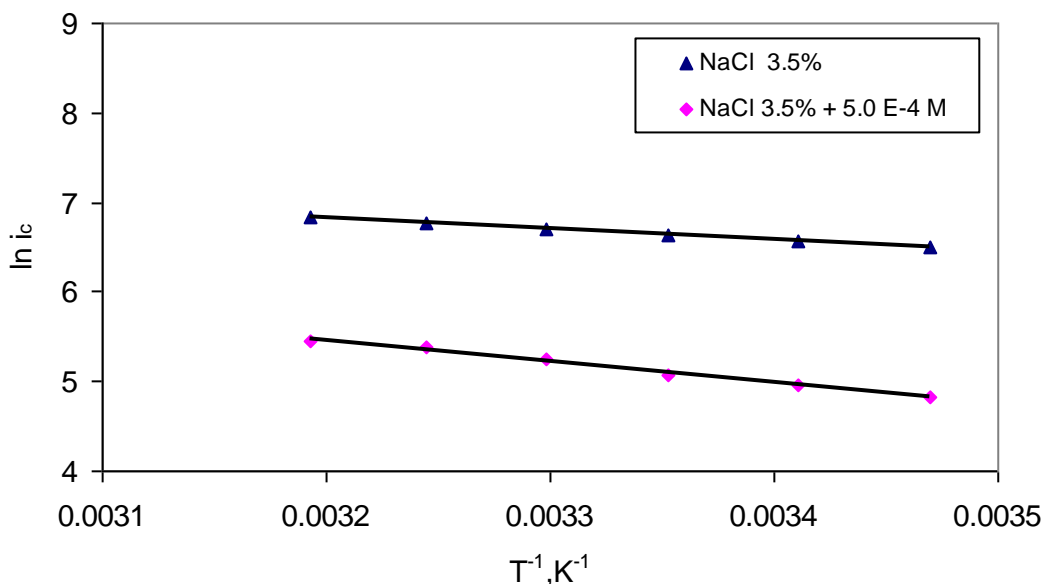


**Figure 2.** Arrhenius-type graph with  $5.0 \times 10^{-4}$  M and without inhibitor

Greater temperature increases corrosion density. The activation parameters of the corrosion process can be calculated from an Arrhenius-type equation:

$$i_c = k \exp - \frac{E_a}{R T} \tag{eq 3}$$

Where  $E_a$  is apparent corrosion activation energy;  $k$  is a pre-exponential Arrhenius factor; and  $T$  is absolute temperature. Using data in Table 2, the activation energy with and without inhibitor can be calculated. For example, the graph in Figure 2 is obtained by using  $5.0 \cdot 10^{-4}$  M inhibitor concentration and plotting  $\ln i_c$  against inverse absolute temperature.

The graph above shows two lines, one with inhibitor and another without it. Their correlation coefficient is close to -1. The activation energy can be calculated from the slopes, 19.4 kJ/mol with inhibitor being slightly higher than 9.95 kJ/mol without inhibitor. This is in agreement with corrosion current density being lower in a system with inhibitor, this also occurs at other concentrations.

### 3.3 Adsorption

An adsorption isotherm describes the equilibrium between the concentration of a certain species in the phase in which it is present and in the metal-electrolyte phase. So, adsorption equilibrium can be written as



where  $\text{ORG}_{(\text{ads})}$  and  $\text{ORG}_{(\text{aq})}$  is the organic compound adsorbed and desorbed at the same speed on the metal surface. The adsorption phenomenon occurs in an aqueous solution containing the organic compound  $\text{ORG}_{(\text{aq})}$ . This involves the displacement of a certain number of water molecules ( $\chi$ ) by the organic compound which is adsorbed on the electrode surface  $\text{H}_2\text{O}_{(\text{ads})}$ .

Inhibitor efficiency ( $I_E$ ) is proportional to the degree surface covering  $\theta$  on the surface of the steel that can have values from 0 to 1 ( $0 \leq \theta \leq 1$ ). The equation that describes a process of adsorption is the adsorption isotherm. The isotherm that is adapted better to the experimental data is the best one. Many isotherms have been developed, some of them theory, and other experimental. Tested isotherms are shown in Table 3, removed from previous work [18]. In general, adsorption isotherm can be expressed as  $K_{\text{ads}}^{\circ} C = \text{function } \theta, f, \chi, h, n$ , where  $K_{\text{ads}}^{\circ}$  is an adsorption equilibrium constant;  $n$  is the number of sites occupied by a molecule of the metal surface;  $f$  represents interactions among adsorbed molecules (this interaction parameter may be positive or negative:  $f < 0$  indicates repulsion force and  $f > 0$  shows lateral attraction among adsorbed organic molecules);  $\chi$  is the substitution of water molecules by an inhibitor molecule; and  $h$  is his measure of adsorption energy distribution in different sites of the surface (this is a heterogeneity parameter ( $0 < h < 1$ )).

To determine the isotherm that fits the experimental data we used the linear correlation coefficient. The isotherm is better adjusted to the experimental data was Flory-Huggins, with  $\chi$  (molecules of water removed from the alloy surface by the adsorbed molecule inhibitor)  $2.4 \leq \chi \leq 3$ . The value must be number whole  $\chi = 3$

Covering coefficients were calculated with Flory-Huggins equation, for example 288.2 K and compared with the experimental one shown in figure 3. This figure shows good agreement between experimental and calculated values.

**Table 3 .** Tested adsorption isotherms

Author	Isotherm	Parameter
<b>Langmuir</b>	$K_{ads}^o C = \frac{\theta}{1-\theta}$	$K_{ads}^2$
<b>Langmuir-Freundlich</b>	$K_{ads}^o C = \left[ \frac{\theta}{(1-\theta)} \right]^{\frac{1}{h}}$	$K_{ads}^2, h$
<b>Langmuir multistity</b>	$K_{ads}^o C = \frac{\theta}{(1-\theta)^n}$	$K_{ads}^2, n$
<b>Frumkin</b>	$K_{ads}^o C = \left( \frac{\theta}{1-\theta} \right) \exp(-f\theta)$	$K_{ads}^2, f$
<b>Hill-de Boer</b>	$K_{ads}^o C = \left( \frac{\theta}{1-\theta} \right) \exp\left( \frac{\theta}{1-\theta} \right) \exp(-f\theta)$	$K_{ads}^2, f$
<b>Parsons</b>	$K_{ads}^o C = \left( \frac{\theta}{1-\theta} \right) \exp\left( \frac{2-\theta}{(1-\theta)^2} \right) \exp(-f\theta)$	$K_{ads}^2, f$
<b>Damaskin-Parsons</b>	$K_{ads}^o C = \frac{\theta}{(1-\theta)^z} \exp(-f\theta)$	$K_{ads}^2, f$
<b>Flory-Huggins *</b>	$K_{ads}^o C = \frac{\theta}{\chi (1-\theta)^z}$	$K_{ads}^2, \chi$
<b>Dhar-Flory-Huggins</b>	$K_{ads}^o C = \frac{\theta}{(1-\theta)^z \exp(\chi-1)}$	$K_{ads}^2, \chi$
<b>Temkin</b>	$K_{ads}^o C = \theta \exp(-f\theta)$	$K_{ads}^2, f$

The adsorption equilibrium constants were determined with the Flory-Huggins isotherm and adsorption free energy was calculated with the expression:

$$\Delta G_{ads}^o = -R T \ln \left( K_{ads}^o 55.55 \right) \tag{eq 4}$$

In table 4 one is summarized the constant and the free energy of adsorption as a function of temperature. In this table it can be seen with increasing temperature, decreasing the adsorption equilibrium constant this indicates that the reaction is exothermic and the sign of the variation of free energy indicates the spontaneous adsorption. The physisorption are consistent with electrostatic interactions between the inhibitor and the charged metal surface, on the other hand chemisorptions as a result of sharing or transfer of electrons from inhibitor molecules to the metal surface to form a coordinate type of bond. Generally, values of free energy adsorption increased to -20 kJ / mol comprises a physisorption and lower values of -40 kJ / mol is associated with a chemisorption [19-28] , according to table 4, the adsorption in this study to be chemisorptions.

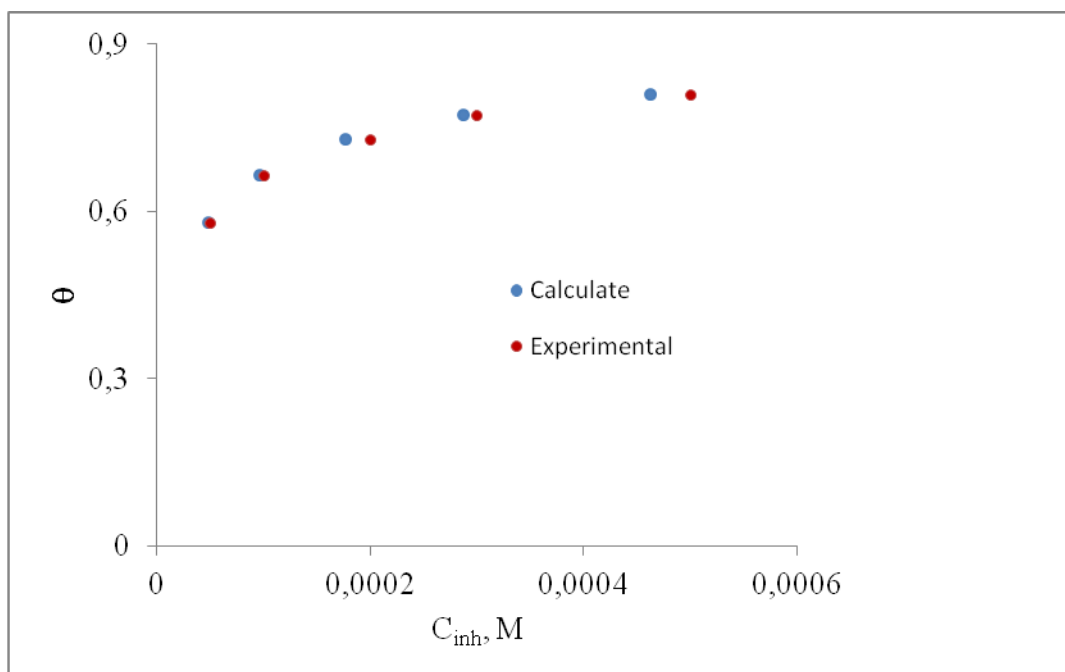


Figure 3. Comparison between experimental and calculated values of  $\theta$  at 288.2 K

Table 4 .Adsorption equilibrium constant variation and  $\Delta G^\circ_{ads}$  as a function of temperature.

Temperature K	$K^0_{ads}$ (dm <sup>3</sup> /mol)	$\Delta G^\circ_{ads}$ (kJ/mol)
288.2	39.76 10 <sup>3</sup>	-35.00
293.2	33.99 10 <sup>3</sup>	-35.23
298.2	31.44 10 <sup>3</sup>	-35.63
303.2	30.70 10 <sup>3</sup>	-36.17
308.2	27.40 10 <sup>3</sup>	-36.48
313.2	25.39 10 <sup>3</sup>	-36.87

When plotted normal adsorption energy variation against temperature, Figure 4 obtained which is adjusted to the polynomial, which has a squared correlation coefficient is close to 1.

$$\Delta G^\circ_{ads} = 11.56 \cdot 10^{-5} T^3 - 10.46 \cdot 10^{-2} T^2 + 31.44 T - 31.78 \cdot 10^2 \text{ kJmol}^{-1} \tag{eq5}$$

As  $\left(\frac{\partial \Delta G^\circ_{ads}}{\partial T}\right)_P = -\Delta S^\circ_{ads}$  is normal adsorption entropy variation, then

$$\Delta S^\circ_{ads} = -34.68 \cdot 10^{-5} T^2 + 20.92 \cdot 10^{-2} T - 31.44 \text{ kJ}(\text{mol K})^{-1} \tag{eq6}$$

Considering that  $\Delta H^\circ_{ads} = \Delta G^\circ_{ads} + T\Delta S^\circ_{ads}$ , we have that

$$\Delta H^\circ_{ads} = -23.12 \cdot 10^{-5} T^3 + 10.46 \cdot 10^{-2} T^2 - 31.78 \cdot 10^2 \text{ kJ mol}^{-1} \tag{eq7}$$

In the rank of tried temperatures it is had

$\Delta G^\circ_{ads} < 0$ ,  $\Delta H^\circ_{ads} < 0$  and  $\Delta S^\circ_{ads} > 0$ , this means that the adsorption process is spontaneous and exothermic.

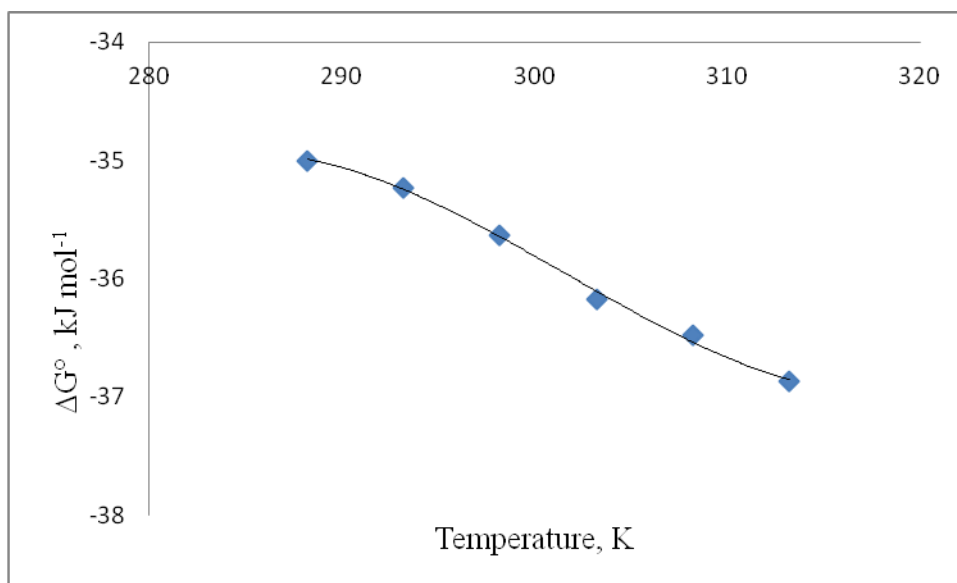


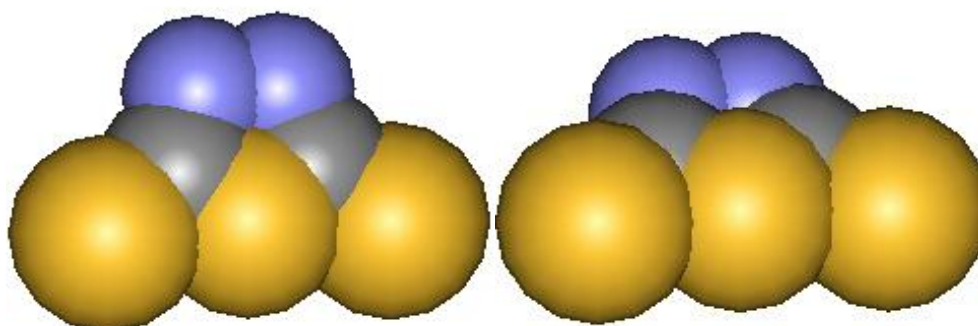
**Figure 4.** Normal free adsorption energy variation with temperature

### 3.4. Molecule projection on surface

The objective is to analyze the possible optimal direction of 1,3,4-thiadiazole-2,5-dithiol on the surface of steel ASTM A890-1B being used the molecular models described in literature [20,30].

A conventional model has been used, in which the atoms are associated as rigid spheres and of that form its surface based on the radii of Van der Waals, the angles of connection and the bond length of [31].

Figure 5 shows the molecule of 1,3,4-thiadiazole-2,5-dithiol in vertical and horizontal form. The program Weblab Viewer Pro 4,0 for the calculation was used areas of adsorption. Being these areas  $\approx 22,1$  and  $\approx 39,5$  ( $\text{\AA}^2$ ) for the surface of vertical and horizontal adsorption respectively. The area occupied by to vertical you adsorb to water molecule is in the range from 8 to 12 ( $\text{\AA}^2$ ) [32].



ASTM A-890-1B Stainless Steel

**Figure 5.** Molecule of 1,3,4-thiadiazole-2,5-dithiol in vertical and horizontal form

The area ratio of adsorption is:

$$\frac{1,3,4\text{-thiadiazole-2,5-dithiol vertical}}{\text{water vertical}} \approx 2.8 \text{ to } 1.8$$

$$\frac{1,3,4\text{-thiadiazole-2,5-dithiol horizontal}}{\text{water vertical}} \approx 2.9 \text{ to } 3.3$$

The thiadiazoles inhibit the corrosion by controlling both the anodic and cathodic reactions. In acidic solutions these compounds exist as protonated species. These protonated species adsorb on the cathodic sites of the mild steel and decrease the evolution of hydrogen. The adsorption on anodic sites occurs through the  $\pi$ -electrons of aromatic rings and lone pair of electrons of nitrogen and sulphur atoms, the molecule could be horizontal. Adsorption of inhibitor molecules are often a displacement reaction involving removal of adsorbed water molecules from the metal surface. So that, during the adsorption of the inhibitor molecules on the metal surface, the change in the interaction energy with water molecules in passing from the dissolved in the adsorbed state form an important part of the free energy change of adsorption process,  $\Delta G^{\circ}_{\text{ads}}$ . The  $\pi$ -electron possibly overlaps with the vacant d-orbital of the surface of iron resulting in a strong  $d\pi-\pi p$  interaction. Surface coverage data. The adsorption the compounds organic on the metal surface can occur either d-orbital of iron surface atoms or an interaction of organic nitrogen compounds with already adsorbed directly on the basis of donor-acceptor interactions between the  $\pi$ -electrons of the ring and the vacant groups [33-35]. Then three water molecules could be displaced by each inhibitor molecule, in agreement with Flory-Huggins isotherm calculation.

#### 4. CONCLUSIONS

- 1, 3, 4-thiadiazole-2, 5-dithiol is a corrosion inhibitor of ASTM A-890-1B steel in a NaCl 3.5% solution.
- The efficiency of inhibitor increases with the increase of the concentration.
- To a same concentration efficiency of inhibitor diminishes when increasing the temperature.
- Activation energy with inhibitor is slightly higher than that without it.
- The inhibitor affects the anodic and cathodic processes, thus showing that the inhibition mechanism is mixed.
- Inhibitor adsorption on ASTM A-890-1B steel surface obeys Flory-Huggins isotherm.
- According to Flory-Huggins isotherm, 3 water molecules are displaced, as proven by surface calculation.
- According to free energy variation signs and normal enthalpy, the adsorption process is spontaneous and exothermic.
- The adsorption in this study to be chemisorption

## ACKNOWLEDGEMENTS

The authors are thankful to the Catholic University of the North with the economic support to make this work.

## References

1. V.S. Sastri. "Corrosion Inhibitors-Principles and Applications", John Wiley and Sons, Chichester,1998.
2. V.S. Sastri, J.R Perumareddi, *Corrosion*, 53 (1997) 617
3. M.Elaiyachy, A.El Idrissi, B.Hammouti, *Corros. Sci.*, 48 (2006) 2470
4. Abd-El-Nabey, E.Khamis, M.Sh. Radaman , A.El-Gindy, *Corrosion*, 52 (2000) 671
5. F.Bentiss, M. Lebrini , M.Lagrenée, *Corros. Sci.*, 47 (2005) 2915
6. M.Abdallah, E.A. Helal, A.S. Fouda, *Corros. Sci.*, 48 (2006) 1639
7. L.Wang, G. J.Yin, Q-F Zhang, J.X .Pu, *Corrosion*, 56 (2000)1083
8. Abd-El-Nabey, E.Khamis, M.Sh. Radaman , A.El-Gindy, *Corrosion*, 52 (2000) 671
9. R.Gasparac , C. Martin, *J. Electrochem. Soc.*, 148(4) (2001) B138- B145
10. M. Guzmán, R.Lara , L. Vera, *J. Chil. Chem. Soc.*, 54 (2009) 123
11. P. Ortega, L. Vera and M. Guzmán, *Macromol. Chem .Phys.*, 198 (1997) 2949
12. D.E.Riple,*Chem.Abtr.*84 (1976)7432k
13. Ger.2,653,568 (1977),Exxon Research and Engineering Co., invs.: S. J. Brois and T. Colclugh;*Chem.Abstr.* 86 (1977) 189960c
14. H.Baeza, M. Guzman, P.Ortega , L. Vera, *J. Chil. Chem. Soc.*, 48(2003) 23
15. E. M. Sherif, Su-Moon Park, *Corros. Sci.*, 48(2006), 4065
16. INTERNATIONAL MOLYBDENUM ASSOCIATION. Practical Guidelines for the Fabrication of Duplex Stainless Steel. 2<sup>th</sup> ed. Pittsburgh, PA, USA, TMR Stainless. 63 (2009)
17. N. Alonso- Falleiros, A. Hakim, S. Wolynech, *Corrosion*, 55(1999) 443
18. J.M. Bastidas, P. Pinilla, J.L. Polo, F. Cano, *Corrosion*, 58(2002), 922
19. C. Das, *Indian J. Chem. Technol.*,3 (1996) 259
20. F.M. Donahue,K. Nobe, *J. Electrochem. Soc.* , 112 (1965) 886
21. B. G. Ateya, B. E. El-Anadouli, F. M. El-Nizamy, *Corros. Sci.*, 24 (1984) 509
22. S.S. Mahmoud, M.M. Ahmed, *Port Electrochim. Acta*, 24(2006) 37
23. J.O. Olusola et al., *Port. Electrochim. Acta*, 27 (2009) 591
24. E.E.Ebenso,N.N.Eddy,and A.O.Odiongenyi,*Port. Electrochim. Acta*,27(2009)13
25. S.A.Umoren,Y.Li,andF.H.Wang, *Corros. Sci.*,52 (2010)1777
26. 26.B.Anand,M.Jayandran,and V.Balasubramanian, *J. Corros. Sci. and Engin.*,15(2012)p18
27. E.B. Ituen,U.E.Udo,N.W.Odozi, and E.U.Dan, *J. Appl. Chem.*,3(2013)52
28. S.Adejo, J. Gbertyo, and J.Ahile, *Int. J. Mod. Chem.*, 4(2013)137
29. H.P. Dhar, B.E. Conway, K.M. Joshi, *Electrochim. Acta*, 18 (1973) 789
30. H.H. Hassan , *Electrochim. Acta*, 51 (2005) 526
31. R. Fuchs-Godec and V. Dolecek , *Acta Chim. Slov.* , 51(2004)495
32. J.M. Bastidas, P. Pinilla, E.Cano,J.L.Polo, and S. Miguel, *Corros. Sci.*, 45(2003) 427
33. M.Z.A. Rafiquee, S. Khan, N. Saxena and M.A. Quraishi, *Port. Electrochim. Acta* 25(2007) 419
34. R.T. Loto, C.A. Loto and A.P.I. Popoola, *J. Mater. Environ. Sci.*, 5(2012) 885
35. H. Amar et. al., *Corros. Sci.* 49(2007) 2936